Lactoferrin is a natural inhibitor of plasminogen activation

Received for publication, March 26, 2018, and in revised form, April 7, 2018 Published, Papers in Press, April 18, 2018, DOI 10.1074/jbc.RA118.003145

Alexander Zwirzitz[‡], Michael Reiter[‡], Rostislav Skrabana[§], Anna Ohradanova-Repic[‡], Otto Majdic[†¶], Marianna Gutekova[‖], Ondrej Cehlar[§], Eva Petrovčíková[‖], Eva Kutejova[‖], Gerold Stanek[‡], Hannes Stockinger[‡], and Vladimir Leksa[‡‖1]

From the [‡]Institute for Hygiene and Applied Immunology and [¶]Institute of Immunology, Center for Pathophysiology, Infectiology, and Immunology, Medical University of Vienna, A-1090 Vienna, Austria and the [§]Laboratory of Structural Biology of Neurodegeneration, Institute of Neuroimmunology, and the [‖]Laboratory of Molecular Immunology, Institute of Molecular Biology, Slovak Academy of Sciences, Bratislava 814 38, Slovak Republic

Edited by George N. DeMartino

The plasminogen system is essential for dissolution of fibrin clots, and in addition, it is involved in a wide variety of other physiological processes, including proteolytic activation of growth factors, cell migration, and removal of protein aggregates. On the other hand, uncontrolled plasminogen activation contributes to many pathological processes (*e.g.* tumor cells' invasion in cancer progression). Moreover, some virulent bacterial species (*e.g. Streptococci* or *Borrelia*) bind human plasminogen and hijack the host's plasminogen system to penetrate tissue barriers. Thus, the conversion of plasminogen to the active serine protease plasmin must be tightly regulated. Here, we show that human lactoferrin, an iron-binding milk glycoprotein, blocks plasminogen activation on the cell surface by direct binding to human plasminogen. We mapped the mutual binding sites to the N-terminal region of lactoferrin, encompassed also in the bioactive peptide lactoferricin, and kringle 5 of plasminogen. Finally, lactoferrin blocked tumor cell invasion *in vitro* and also plasminogen activation driven by *Borrelia*. Our results explain many diverse biological properties of lactoferrin and also suggest that lactoferrin may be useful as a potential tool for therapeutic interventions to prevent both invasive malignant cells and virulent bacteria from penetrating host tissues.

The plasminogen activation system plays a fundamental role in dissolution of fibrin clots. However, the active serine protease plasmin, a central player of the system, is in addition employed in a plethora of physiological processes, such as the proteolytic activation of growth factors and pro-metalloproteinases, cell migration, and the removal of protein aggregates. Moreover, a variety of human pathologies are associated with the imbalanced plasminogen activation (*e.g.* tumor cells' dissemination (1), neurodegeneration (2), and various inflammatory disorders (3)).

The conversion of plasminogen (Plg)[2] to plasmin is catalyzed by several enzymes. First, the tissue-type plasminogen activator is responsible for proteolytic activation of Plg on the extracellular matrix required for the resolution of blood clots. Second, the urokinase-type plasminogen activator (uPA) is the central serine protease for Plg activation by migratory cells, such as activated leukocytes, endothelial cells, and fibroblasts, but also tumor cells. Upon binding to the urokinase-type plasminogen activator receptor (uPAR, CD87), inactive pro-urokinase is processed to active uPA, which in turn specifically converts cell-bound Plg to plasmin. The uPA/Plg system might be also hijacked by bacterial species (*e.g. Borrelia burgdorferi*) which contributes to their virulence (4, 5). In addition, *Streptococcus pyogenes* secrets streptokinase (SK) capable of binding one Plg molecule to convert another Plg molecule to plasmin independently of the host's uPA (6).

On the other hand, there are several ways to keep Plg activation under control. First, uPA is susceptible to the inhibition by plasminogen activator inhibitors (*e.g.* PAI-1); second, direct plasmin inhibitors (*e.g.* α2-antiplasmin) are present in the plasma and rapidly inactivate unbound plasmin; and third, Plg interacts, typically via lysine-binding sites located in its kringle domains, with lysines encompassed in receptors, which restricts Plg activation on the cell surface.

Here, we identify the milk immunomodulatory glycoprotein lactoferrin (LF), also known as lactotransferrin, as a natural and specific inhibitor of the uPA-mediated plasminogen activation. LF is an iron-binding glycoprotein from the family of transferrins. The main source of human LF is human milk, secondary granules of neutrophils, and it is present also in

This work was supported by Austrian Science Fund Grants P19014-B13, P22908, and I00300; Science and Technology Assistance Agency of the Slovak Republic Grant APVV-16-0452; Slovak Grant Agency VEGA Grant 2/0020/17; the European Union Seventh Framework Program (FP7/2007–2013) under grant agreement NMP4-LA-2009-228827 NANOFOL; and the EU structural funds ITMS 26240220008. The research was also supported by the European Union's Horizon 2020 Research and Innovation Program under Grant Agreement 683356 (FOLSMART). The authors declare that they have no conflicts of interest with the contents of this article.

This work is dedicated to Professor Otto Majdic.

[†] Deceased February 9, 2018.

[1] To whom correspondence should be addressed: Institute for Hygiene and Applied Immunology, Center for Pathophysiology, Infectiology, and Immunology, Medical University of Vienna, Lazarettgasse 19, A-1090 Vienna, Austria. Tel.: 43-1-40160-33006; Fax: 43-1-40160-933002; E-mail: vladimir.leksa@meduniwien.ac.at.

[2] The abbreviations used are: Plg, plasminogen; BN-PAGE, blue native polyacrylamide gel electrophoresis; DLS, dynamic light scattering; LF, lactoferrin; LFC, lactoferricin; M6P, mannose 6-phosphate; IGF2R, insulin-like growth factor 2 receptor; mAb, monoclonal antibody; SK, streptokinase; SPR, surface plasmon resonance; TF, transferrin; uPA, urokinase-type plasminogen activator; uPAR, urokinase-type plasminogen activator receptor; HUVEC, human umbilical vein endothelial cell; TEMED, *N*,*N*,*N*′,*N*′-tetramethylethylenediamine; HRP, horseradish peroxidase; Ab, antibody; cfu, colony-forming unit(s); PDB, Protein Data Bank; AF647, Alexa Fluor 647.

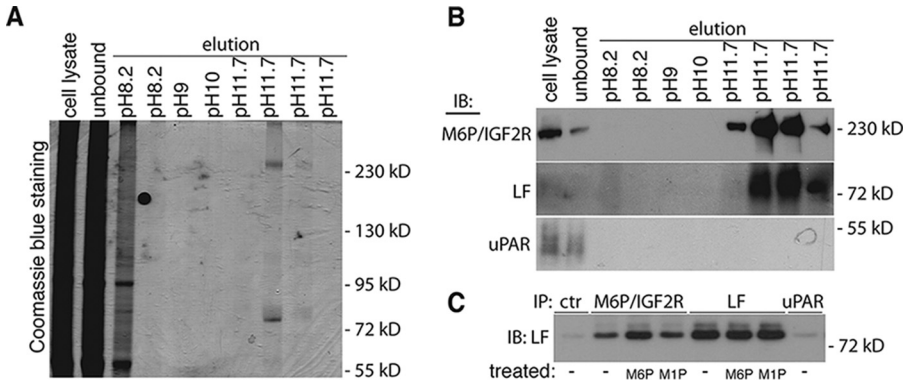

Figure 1. LF interacts with M6P/IGF2R. *A*, the fractions of M6P/IGF2R purified by affinity chromatography were analyzed by SDS-PAGE. The ~80 kDa Coomassie-stained gel band co-purified with M6P/IGF2R was cut for LC-MS/MS analysis. *B*, the fractions were analyzed by immunoblotting (*IB*) using mAbs to M6P/IGF2R (MEM-238), LF (4C5), and uPAR (H2). *C*, the human granulocyte cell lysate, obtained with 1% Triton X-100 together with 0.5% dodecylmaltoside as detergents, was subjected to immunoprecipitation on a 96-well plastic plate (50 μl/well) coated with goat anti-mouse IgG (5 μg/ml) and specific antibodies to M6P/IGF2R (mAb clone MEM-238), LF (mAb clone 4C5), and uPAR (mAb clone H2); as isotype control, mAb AFP-01 was used (*ctr*) (all 5 μg/ml). The incubation was performed for 4 h at 4 °C in the presence or absence of mannose 1-phosphate (*M1P*) and M6P (both 10 mmol/liter). The precipitates were analyzed by SDS-PAGE followed by immunoblotting using the specific mAb to LF (LF95-4C5).

serum and exocrine secretions. Antimicrobial, antitumor, and immunomodulatory activities have been attributed to LF (7, 8). Here, we demonstrate a so far unknown function of LF in regulation of fibrinolysis and unravel the molecular determinants and mechanism whereby lactoferrin blocks plasminogen activation.

Results

Our previous studies demonstrated that the mannose 6-phosphate/insulin-like growth factor 2 receptor (M6P/IGF2R, CD222) binds and internalizes Plg (9–12). To get a better insight into the underlying molecular mechanisms, we sought further ligands of M6P/IGF2R. We purified M6P/IGF2R (molecular mass ~300 kDa) by affinity chromatography from the lysate of human monocytic THP-1 cells and co-isolated an ~80-kDa protein (Fig. 1*A*). A trypsin in-gel digestion followed by nano-electrospray MS analysis revealed 25 peptide sequences identical to human LF (Table 1). Besides LF, other proteins with molecular mass ranging from 70 to 90 kDa were identified (Table 2), including Plg and GlcNAc-6-sulfatase, both known ligands of M6P/IGF2R (9, 13).

The Western blot analysis confirmed the specificity of LF (Fig. 1*B*). We verified the interaction further by co-immunoprecipitating LF with M6P/IGF2R from human granulocytes, which are known to produce high amounts of LF (Fig. 1*C*). M6P, which was found in LF (14), did not significantly influence the interaction between LF and M6P/IGF2R, suggesting that the M6P-binding sites in M6P/IGF2R were not required for the interaction (Fig. 1*C*). These findings were proven by an *in vitro* binding assay wherein M6P did not block the interaction, similarly to soluble uPAR (Fig. 2*A*). In contrast, the presence of Plg, a M6P/IGF2R ligand (9), enhanced the weak interaction between LF and M6P/IGF2R (Fig. 2*A*). Based on the latter finding, we tested the possibility of a direct LF-Plg binding. Indeed, an *in vitro* binding assay revealed the direct binding of LF and Plg (Fig. 2*B*).

To map the determinants responsible for the LF-Plg binding, we designed three peptides: pLF1 derived from the N-terminal end of LF and encompassed within lactoferricin (LFC), a small bioactive fragment with anti-pathogenic activity (15); pLF2 derived from the helix linker region of LF encompassing a stretch of lactoferrampin, another bioactive peptide (16); and pLF3 made up of the C-terminal part containing a C-terminal lysine (Table 3), because C-terminal lysines are generally known to be involved in Plg binding (17). We found that pLF1 blocked the binding of LF and Plg with an IC_{50} of about 6 μg/ml (2.8 μM) (Fig. 2, *C–E*). The lysine analogue tranexamic acid (*TA*), which is known to block the lysine-dependent Plg binding, did not have significant effects on the binding as well as the other peptides. This indicates that the Plg-binding site is encompassed within the N-terminal part of LF.

Table 1

MS analysis of the 80-kDa protein band co-purified with M6P/IGF2R

Peptides matched to LF (Mascot protein score = 613). M6P/IGF2R was purified with the anti-M6P/IGF2R mAb MEM-240 from lysates of THP-1 cells. The 80 kDa band co-purified with M6P/IGF2R was excised from the gel for MS/MS analysis. Identification was performed by MASCOT and the NCBI non-redundant protein database. Peptides identified to match to LF are listed.

LF residues	Peptide	Observed mass	Predicted mass
		Da	*Da*
23–39	RRSVQWCAVSQPEATKC	1,745.85	1,747.13
93–107	KLRPVAAEVYGTERQ	1,459.78	1,460.41
108–120	RTHYYAVAVVKK	1,149.62	1,149.36
119–134	KKGGSFQLNELQGLKS	1,517.82	1,518.46
120–141	KGGSFQLNELQGLKSCHTGLRR	2,088.02	2,086.91
171–184	RFFSASCVPGADKG	1,284.58	1,284.88
220–231	RDGAGDVAFIRE	1,019.5	1,019.56
269–279	RVPSHAVVARS	934.53	935.02
283–293	KEDAIWNLLRQ	1,128.59	1,128.95
364–377	RVVWCAVGEQELRK	1,444.71	1,445.24
406–425	KGEADAMSLDGGYVYTAGKC	1,803.8	1,803.2
424–437	KCGLVPVLAENYKS	1,361.7	1,362.15
462–475	RRSDTSLTWNSVKG	1,392.7	1,393.28
504–521	KFDEYFSQSCAPGSDPRS	1,861.76	1,862.15
520–537	RSNLCALCIGDEQGENKC	1,806.79	1,807.25
544–554	RYYGYTGAFRC	1,096.5	1,096.98
553–567	RCLAENAGDVAFVKD	1,392.67	1,392.68
566–585	KDVTVLQNTDGNNNEAWAKD	1,987.92	1,989.08
587–600	KLADFALLCLDGKR	1,334.69	1,335.19
607–623	RSCHLAMAPNHAVVSRM	1,664.79	1,665.55
628–640	RLKQVLLHQQAKF	1,304.79	1,305.38
642–660	RNGSDCPDKFCLFQSETKN	2,031.87	2,032.26
658–673	KNLLFNDNTECLARL	1,578.75	1,579.54
681–696	KYLGPQYVAGITNLKK	1,535.83	1,536.33
681–697	KYLGPQYVAGITNLKKC	1,663.93	1,664.75

Table 2

MS analysis of the 80-kDa protein band co-purified with M6P/IGF2R: Protein hits

M6P/IGF2R was purified with the anti-M6P/IGF2R mAb MEM-240 from lysates of THP-1 cells. The 80 kDa band co-purified with M6P/IGF2R was excised from the gel for MS/MS analysis. Identification was performed by MASCOT and the NCBI non-redundant protein database. Analysis revealed several proteins with the predicted molecular mass ranging from 70 to 90 kDa.

Protein name	NCBI GI number	Predicted mass	Mascot score	Queries matched
		kDa		
Lactoferrin	18490850	80	613	41
ATP-dependent DNA helicase II	4503841	70	448	26
Hydroxysteroid (17-β) dehydrogenase 4	4504505	80	329	12
RNase L inhibitor	3273417	68	266	13
Gastrin-binding protein	595267	84 (78)[a]	172	14
Plasminogen[b]	27806815	94	147	12
Replication protein A1	4506583	69	108	4
Heat shock protein 70	386785	70	107	4
Lamin B1	5031877	66	91	9
N-Acetylglucosamine-6-sulfatase precursor (glucosamine-6-sulfatase)	4504061	63 (100)[a]	88	4
Nucleolin	189306	76 (105)[a]	70	2
Moesin	4505257	68	57	3

[a] The apparent molecular mass in SDS-PAGE.
[b] Species of all proteins were identified as *Homo sapiens* with the exception of plasminogen (*Bos taurus*), indicating that the plasminogen molecule co-purified with M6P/IGF2R was derived from the fetal calf serum used for supplementing the culture medium.

To map the determinants responsible for binding of Plg to LF, we applied fragments derived from Plg generated as described previously (18): angiostatin, consisting of kringle domains 1–4; mini-Plg containing kringle 5 and the proteolytic domain; and micro-Plg encompassing just the proteolytic domain. LF bound strongest to mini-Plg, although we detected a weak binding to all fragments (Fig. 2, *F* and *G*). Upon a higher stringency (*i.e.* in the presence of 0.1% detergent Triton X-100), LF bound only to mini-Plg (Fig. 2*F*). These findings indicate that the major LF-binding site is encompassed within kringle 5 of Plg.

In the next steps, we quantified the binding of LF and Plg by surface plasmon resonance (SPR). To preserve the surface of LF as much as possible, we opted for its immobilization on a streptavidin sensor chip, which facilitated a flexible attachment following biotinylation of the oligosaccharides present at Asn^{147} and Asn^{478} in the N- and C-terminal lobe of LF, respectively (19). Kinetic analysis revealed that LF and Plg formed a high-affinity complex with the dissociation constant equal to 69 $\pm$ 24 nM (Table 4 and Fig. 3*A*).

Interestingly, the SPR profile of Plg association and dissociation gives the best fit to a two-state reaction model (Fig. 3*A*). According to this model, the proteins initially form a metastable complex 1, which is rearranged on a millisecond time scale to a final, slowly dissociating complex 2 (Table 4). To verify the two-state reaction model, we examined dissociation of the LF-Plg complex in two separate SPR experiments, comparing short (60-s) and prolonged (300-s) Plg association time. Indeed, in the experiment with prolonged association time, we detected the formation of a higher amount of the slowly dissociating complex 2 (data not shown), which ultimately confirmed the two-step interaction mechanism.

A freshly prepared LF sensor chip had a very low capacity to bind Plg and required activation by three consecutive 6-s pulses of 100 mM HCl. The sensor chip response decreased by 100 response units during the treatment, but the LF surface became fully competent to interact with Plg and maintained an unchanged reactivity over 1 month of running experiments.

This surprising observation prompted us to investigate the underlying reasons. As the LF-bound iron might be depleted during activation with the acid (20), at first, we tested whether the resaturation of LF with iron could influence Plg binding. However, no change in complex formation was found; therefore, iron presence had no direct influence on the binding.

Second, we examined the oligomeric state of biotinylated LF used in the sensor chip preparation, as LF is able to form tightly bound dimers in diluted solutions at physiologic pH (21), which might influence the Plg binding. We measured molecular radius by dynamic light scattering (DLS) and found that biotinylated LF preparation exhibited a higher average particle size than the initial protein (Table 5), with the weight-averaged molar mass of biotinylated LF corresponding prevalently to the dimeric form (177 kDa *versus* 106 kDa of native LF). The amount of high-molecular weight aggregates was negligible. It suggests that the unresponsiveness of the fresh LF surface might reflect the LF dimerization during labeling, which had occluded surface patches needed for the interaction with Plg. The dimerization of LF occurs also at physiological conditions (22) and may represent a mechanism to control its interaction with Plg.

Each of the three proteins, sM6P/IGF2R, Plg, and LF, had been detected in human serum (23–26). We found that LF co-immunoprecipitated with both sM6P/IGF2R and Plg in human serum (Fig. 3*B*). In addition, blue native electrophoresis analysis (BN-PAGE) implied the presence of several complexes associated with LF in serum (Fig. 3*C*); the low molecular weight species seemed to contain exclusively LF and very likely corresponded to dimers that did not bind Plg as described above; the intermediate diffused complex(es) <272 kDa contained apparently both LF and Plg; the intermediate diffused complex(es) of ~500 kDa contained apparently predominantly sM6P/IGF2R, as shown previously (12); and the high molecular weight complex(es) of >880 kDa appeared to contain Plg, LF, and sM6P/IGF2R (Fig. 3*C*, *arrowheads*). These data suggest that LF may co-exist with Plg in serum in native complexes.

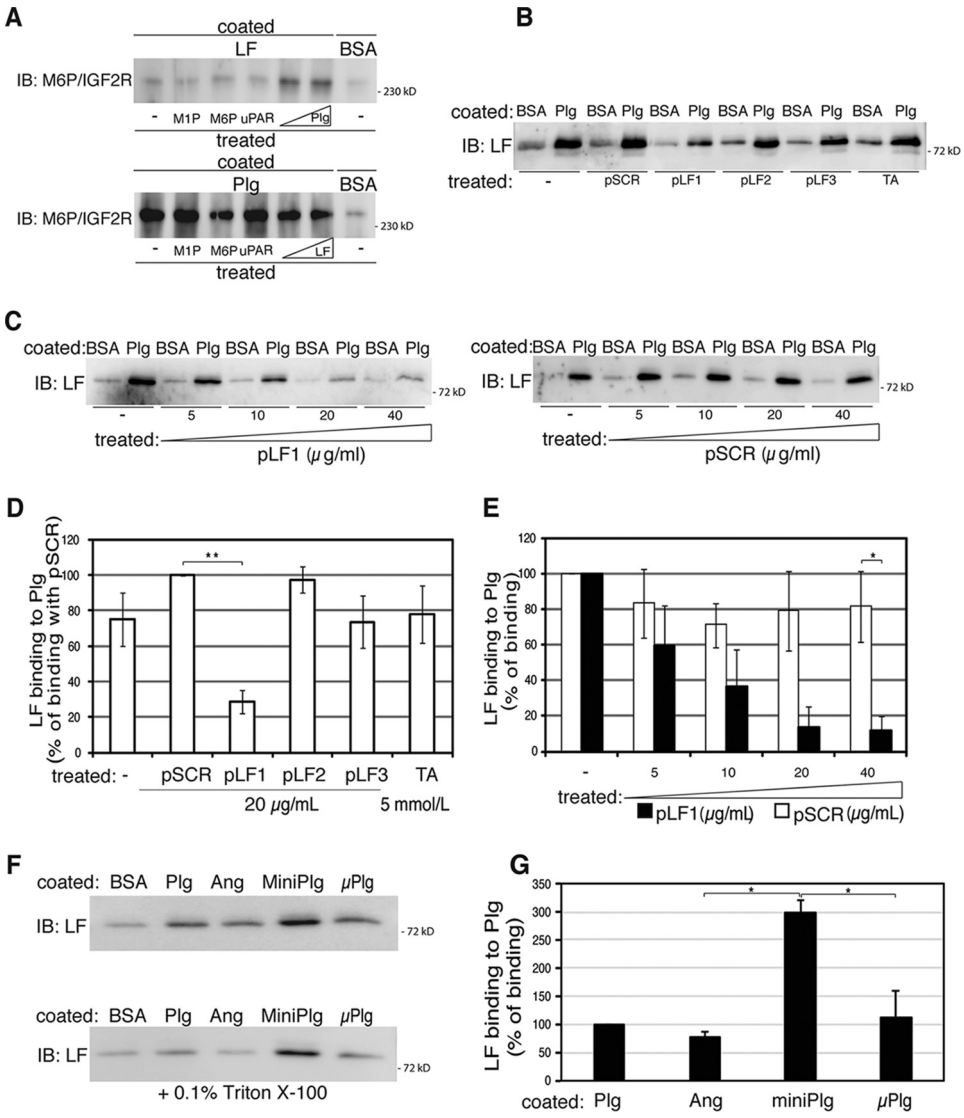

Figure 2. LF interacts with Plg. *A*, LF, Plg, and BSA (as a negative control), coated on wells of a plastic plate (5 μg/ml), were incubated for 4 h on ice with purified M6P/IGF2R (5 μg/ml) in the absence or presence of additional molecules: mannose 1-phosphate (*M1P*) and M6P (both 10 mmol/liter), soluble uPAR (5 μg/ml), Plg (50 and 100 nmol/liter), or LF (20 and 40 μg/ml). Bound material was analyzed by immunoblotting (*IB*) using the specific mAb MEM-238 to M6P/IGF2R. *B*, coated Plg or BSA (5 μg/ml) was incubated for 4 h on ice with LF (20 μg/ml). Before LF was added, some wells were pre-incubated for 2 h on ice with 20 μg/ml LF-derived peptides (pLF1, pLF2, or pLF3) and scrambled peptide (pSCR) or 5 mmol/liter tranexamic acid (*TA*). Bound material was analyzed by immunoblotting using human LF-specific mAb 4E2. *C*, the binding assay was performed as in *B* but with the pre-incubation with increasing concentrations of pLF1 or scrambled peptide pSCR as indicated. *D* and *E*, densitometric quantifications of LF binding assays. A representative immunoblot is shown in *B* and in *C* and *D*, respectively. *Bars*, relative means with S.D. (*error bars*) of at least three independent experiments. The scrambled peptide pSCR served as a control, and the corresponding bands were set as a relative maximum of 100%. Immunoblots were quantified with Fuji MultiGauge software. Bands corresponding to LF binding to BSA were subtracted from the bands of LF binding to Plg bands; in addition, a background correction for each individual lane was applied. The relative IC_{50} value was determined by a 4PL nonlinear regression curve fit, in accordance with National Institutes of Health assay guidance (64). Curve fitting was performed with MasterPlex ReaderFit, published by the MiraiBio Group of Hitachi Software Engineering America, Ltd. *F*, the binding assay was performed as in *B*, but Plg and the Plg fragments angiostatin, mini-Plg, and micro-Plg, or BSA, were coated onto plastic wells. Optionally, the binding assay was performed in the presence of Triton X-100 (0.1%). *G*, densitometric quantification was performed as in *D* and *E*. A representative immunoblot is shown in *F*, without the detergent; *, $p < 0.05$; **, $p < 0.005$.

Table 3
Sequences of the LF-derived peptides

Name	Location	Sequence	Length
pLF1	N-terminal	GRRRSVQWCAVSQPEATKC	19 amino acids
pLF2	Middle	EDAIWNLLRQAQEKFGKDK	19 amino acids
pLF3	C-terminal	NLKKCSTSPLLEACEFLRK	19 amino acids
pSCR	Scrambled	NFRTKSCPLELAKELKLCS	19 amino acids

Next, we tested whether binding of LF to Plg could interfere with Plg activation. First, we found that pre-incubation with LF abrogated AF647-labeled Plg binding to THP-1 cells (known to express high levels of uPAR and uPA (11)) in a concentration-dependent manner with the maximal inhibition (52%) at the concentration of 50 μg/ml (Fig. 4*A*). We analyzed only the binding to viable cells. Second, when the cells were subjected to a Plg activation assay, we found a concentration-dependent inhibitory effect of LF with maximal inhibition at a concentration of 10 μg/ml (Fig. 4*B*). This effect was independent of M6P/IGF2R, previously identified by us to bind and internalize Plg (9, 11), because in both control and M6P/IGF2R-silenced THP-1 cells, generated previously by us (11), a similar effect was

Table 4

Kinetics and affinity of LF-Plg binding

The data are averaged from four independent experiments and expressed as mean ± S.D. k_{ON}, association rate constant of the initial complex formation; k_{OFF1}, dissociation rate constant of the initial complex 1 breakup; k_{ONconf}, rearrangement rate constant; k_{OFF2}, dissociation rate constant of the final complex 2; K_D, equilibrium dissociation constant.

k_{ON}	k_{OFF1}	k_{ONconf}	k_{OFF2}	K_D
$M^{-1}\,s^{-1}$	s^{-1}	s^{-1}	s^{-1}	M
$(8.6 \pm 1.5) \times 10^5$	0.15 ± 0.02	$(9.6 \pm 0.5) \times 10^{-3}$	$(6.2 \pm 1.4) \times 10^{-3}$	$(6.9 \pm 2.4) \times 10^{-8}$

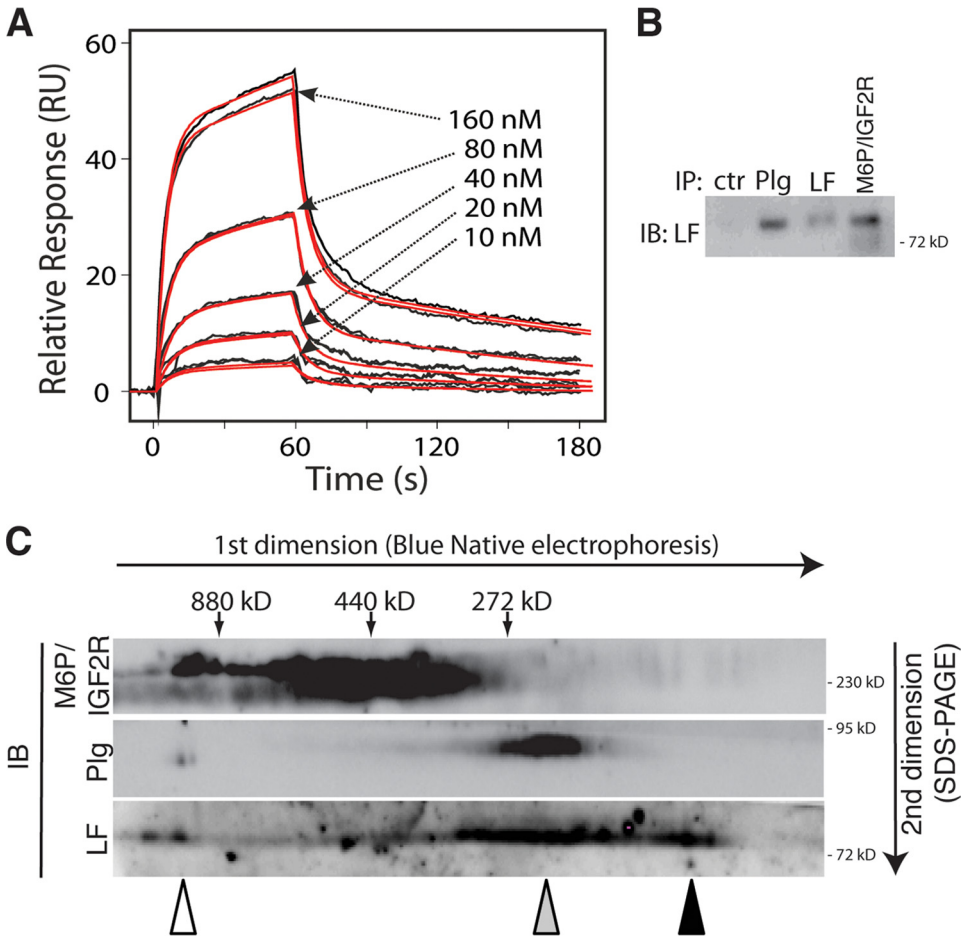

Figure 3. Biochemical analysis of the LF-Plg complex. *A*, SPR analysis of LF-Plg binding. Duplicates of serially diluted Plg at the indicated concentrations were injected over immobilized LF, and the SPR response was fitted to a 1:1, two-state reaction model. *Black traces*, experimental response; *red traces*, fitted response. *B*, LF complexes with Plg and sM6P/IGF2R in serum. To analyze human serum, samples were diluted 20× with PBS and subjected to immunoprecipitation (*IP*) on a 96-well plastic plate via goat anti-mouse IgG and specific antibodies to M6P/IGF2R (MEM-238), LF (LF95–4C5), and Plg (7Pg); as an isotype, control mAb AFP-01 was used (*CTR*). The precipitates were analyzed by SDS-PAGE followed by immunoblotting (*IB*) using biotinylated polyclonal Ab to LF and streptavidin-HRP conjugate. *C*, analysis of LF-Plg complexes in serum. A serum sample (10× diluted) was analyzed by BN-PAGE in the first dimension followed by SDS-PAGE in the second dimension, as described under "Experimental procedures." Then the immunoprecipitates were analyzed by immunoblotting using biotinylated mAb to M6P/IGF2R (MEM-238), biotinylated polyclonal Ab to LF, or mAb 7Pg to Plg followed by streptavidin-HRP conjugate or HRP-conjugated goat anti-mouse IgG secondary antibody. *Arrows*, molecular weight standards. The *open*, *gray*, and *closed arrowheads* indicate the high, intermediate, and low molecular species of LF complexes.

observed: 75 and 82% inhibition, respectively. However, M6P/IGF2R-silenced cells displayed a 30% higher capacity to activate Plg compared with control cells (Fig. 4*B*), which was in line with our previous work showing the M6P/IGF2R-dependent negative regulation of Plg activation by means of the stable genetic knockout and knockdown experiments (10, 11). Third, by a cell-free system, we found that LF hampered Plg activation on coated uPA in a concentration-dependent manner with an IC_{50} value of 3 μg/ml (43 nM), similarly to the plasmin inhibitor aprotinin (Fig. 4*C*). An *in vitro* binding assay revealed that LF completely blocked the binding of Plg to uPA at a concentration of 10 μg/ml (Fig. 4*D*), which is in agreement with its effect on Plg activation.

Finally, we performed an *in vitro* binding assay in the presence of mAbs specific to both LF and Plg, and we found that the anti-LF mAb 1D2 blocked the interaction between LF and Plg (Fig. 5*A*). A pre-incubation of LF with mAb 1D2 abrogated the inhibition of Plg activation by LF at a concentration of 20 μg/ml (Fig. 5, *B* and *C*).

We also tested whether LF was able to block Plg activation by purified SK, a protein secreted by *Streptoccoci* that binds and activates Plg independently of uPA (27, 28). We found that LF

Table 5
LF size analysis by light scattering
The data are expressed as mean ± S.D. MW-S, molecular mass derived from static light scattering of sample; MW-Rm weight-averaged hydrodynamic molar mass derived from autocorrelation function by cumulant analysis; NA, not available; ND, not detected.

	Native LF	Biotinylated LF
c (mg/ml)	9	0.1 – 0.2
MW-S (kDa)	89.1 ± 1.2	NA
Hydrodynamic radius (nm)	4.37 ± 0.06	5.44 ± 0.19
Polydispersity (%)	11.9 ± 3.9	> 50 (multimodal)
MW-R (kDa)	106.0 ± 3.2	177 ± 15
Aggregates >50 nm (mass %)	ND	0.8 ± 0.2

did not have any inhibitory effect on Plg activation by SK (Fig. 4*E*). Together, these results suggest that LF inhibits plasmin generation on the surface of cells through a blockade of Plg binding to uPA.

LF is an iron-binding glycoprotein and a member of the lactotransferrin family. However, we did not observe any inhibition of Plg activation by human transferrin (TF) (Fig. 4*F*). Although LF is structurally highly similar to TF (29), the superimposed structure comparison of LF and TF showed that their N-terminal parts possessed several distinctions very likely caused by the presence of several positively charged amino acid residues within LF not present in TF (*e.g.* an N-terminal stretch of arginines) (Fig. 6, *A* (*arrow*), *B*, and *C*). Because we mapped the Plg-binding site into this N-terminal part of LF (Fig. 2, *B–E*), these differences might be decisive in a contrasting capability of LF and TF to block Plg activation. This finding further underlines the specificity of the LF-mediated inhibition of Plg activation.

In the last series of experiments, we tested the effect of LF on patho/physiological processes associated with the Plg system. The Plg system is utilized by migratory cells to penetrate tissues (*e.g.* endothelial cells during angiogenesis harness uPA-dependent Plg activation) (30, 31). However, tumor cells also activate Plg by uPA, which contributes to their dissemination (32). Accordingly, we performed *in vitro* Matrigel cell invasion assays by using the kidney carcinoma cell line TCL-598 and primary human umbilical vein endothelial cells (HUVECs), both shown by us previously to migrate in a uPA/Plg-dependent manner (10, 12). We found that LF reduced the invasiveness of both TCL-598 cells and HUVECs (Fig. 7, *A* and *B*). Thus, LF can exert negative regulatory effects on cell migration via inhibition of Plg activation.

Also virulent bacteria hijack the Plg system to increase their invasiveness. For instance, *Streptococci* secret SK, which on the one hand binds one "enzyme" Plg molecule and on the other hand activates another "substrate" Plg molecule in a uPA-independent manner (27, 33). In contrast, *Borrelia* do not produce any intrinsic Plg activator; instead, they bind and employ components of the host's fibrinolytic system, namely Plg and uPA, via outer surface proteins (4, 5, 34, 35) to penetrate the host. Thus, we tested the ability of LF to inhibit Plg activation by *B. burgdorferi* and *S. pyogenes*. When we incubated human serum with *B. burgdorferi* and the plasmin-specific chromogenic substrate, we observed a blockade of Plg activation by LF (Fig. 7*C*). In contrast, in the presence of *S. pyogenes*, LF did not reduce Plg activation (Fig. 7*D*). This observation was in line with the above-mentioned experiments with purified enzymes showing that LF was able to inhibit Plg activation by uPA but not SK (Fig. 4). Taken together, these results show that LF can modulate patho/physiological processes of Plg, such as tumor cell invasion and invasion of certain bacteria.

Discussion

LF is known to display a plethora of antimicrobial properties and antitumor activities (7). Its iron binding ability and the unique positively charged N-terminal region are considered to explain most of its biological activities (8). Here, we identified a so far unknown function of LF; it binds Plg and blocks its activation by uPA but not by bacterial SK.

We identified the interaction by means of MS analysis of the proteins co-immunoprecipitated with M6P/IGF2R. This suggests that M6P/IGF2R, a Plg receptor, might be involved in effects of LF. In this respect, it is of interest that M6P/IGF2R is required for herpes simplex virus type 1 infection (36), and LF inhibits herpes simplex infection and trafficking (37). Moreover, also nucleolin, another protein identified by us as a partner of M6P/IGF2R (Table 2), seems to be involved in herpes simplex virus type 1 infection (38). The putative functional network among M6P/IGF2R, LF, and herpes simplex virus remains a topic for future study.

Here, we mapped the mutual binding sites of LF and Plg within the N-terminal region of LF and kringle 5 of Plg, respectively. We show that through this interaction, LF controls Plg activation. We propose that LF inhibits Plg activation on cells via the blockade of the Plg-uPA interaction, which is in agreement with the observation that the majority of lysine-dependent Plg binding to the cell surface depends on the presence of uPA (39). However, it is also possible that LF via binding to Plg blocks a conformational conversion of Plg (40) required for its activation.

LF shares significant sequence and structural homology with TF, a further member of the iron-binding transferrin family. However, TF does not possess the inhibitory activity of LF toward Plg, which might be due to the different composition within their N termini.

Plg is an inactive zymogen circulating in plasma at relatively high concentration (2 μM) (23, 41). Plg binding to the matrix protein fibrinogen (K_D = 0.32 μM) is required for conversion of Plg to active plasmin during blood clot resolution (42). In addition, Plg binds with K_D values ranging from 0.1 to 2 μM also to various cell surface receptors, which is indispensable for cell migration (17, 39, 43). Both pathways (*i.e.* Plg activation on the clots and on the cellular surface) are mediated by Plg activators, tissue-type plasminogen activator and uPA, respectively (32). Strikingly, Plg binds with higher affinity (K_D = 420 pM) to bacterial SK (44–46). SK is a Plg activator employed by invasive human pathogens to facilitate their spreading through host barriers (27, 28). Plg activators are susceptible to inhibition by specific plasminogen activator inhibitors. Also, direct plasmin inhibitors are present in plasma and rapidly inactivate free unbound plasmin (*e.g.* α2-antiplasmin binds to various Plg types with K_D values ranging from 0.2 to 1.9 μM) (47–50).

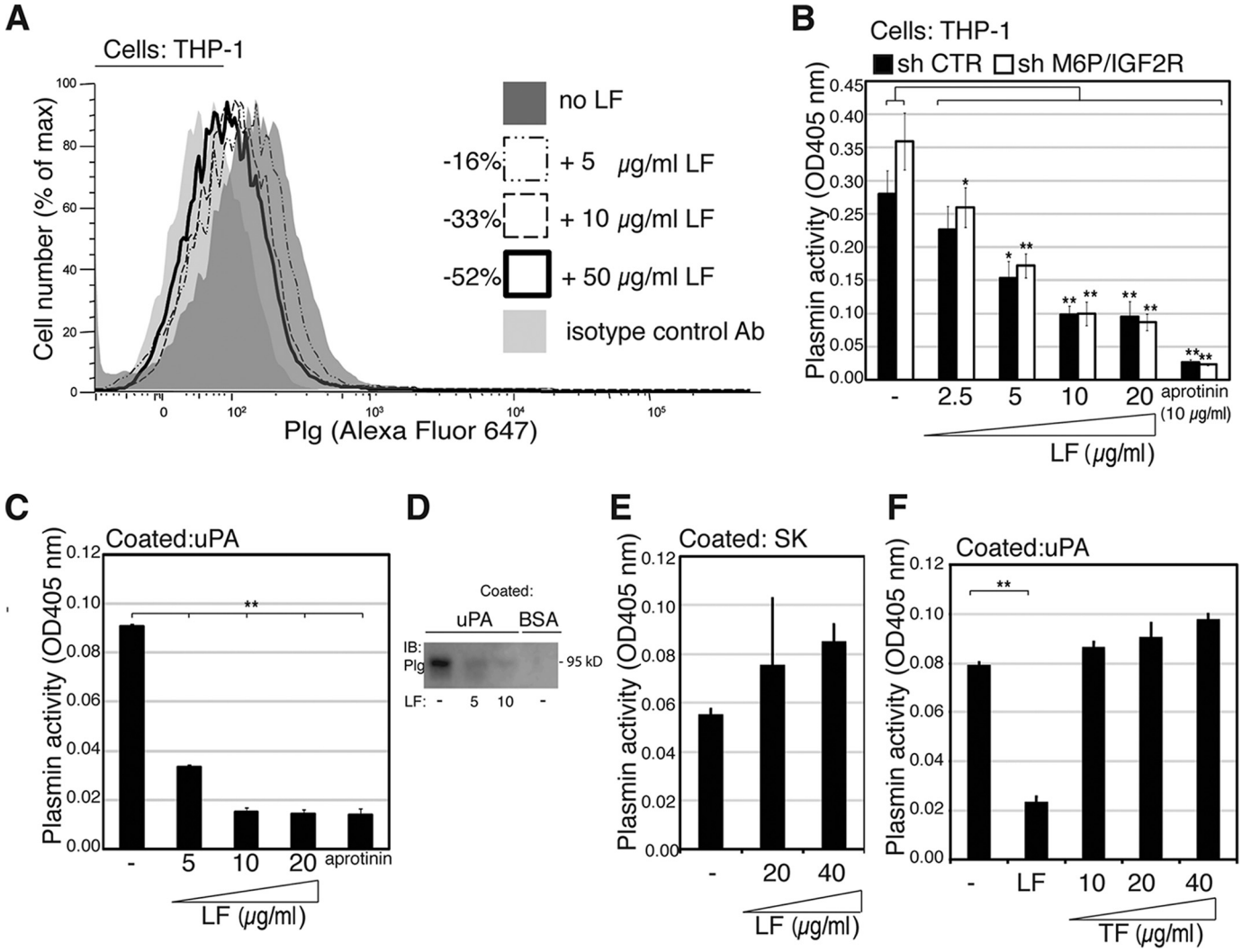

Figure 4. LF blocks Plg activation by uPA. *A*, to measure Plg binding to cells, Plg-AF647 (10 μg/ml) was pre-incubated on ice for 30 min with or without LF at the indicated concentrations. Then THP-1 cells were incubated on ice for 20 min with the Plg preparations, and the cell surface–bound Plg was analyzed by flow cytometry. Histograms are representative of three experiments. The values show the percentage of differential mean fluorescence intensity. The anti-mouse IgG-AF647 conjugate was used as a negative control. *B*, both control and M6P/IGF2R-silenced THP-1 cells were incubated at 37 °C in serum-free medium together with Plg (50 nmol/liter) and the chromogenic plasmin substrate S-2251 (0.8 mmol/liter) in a 96-well plate (5×10^5 cells/well). The reactions were performed with or without LF or aprotinin at the indicated concentrations. The absorbance change at 405 nm was monitored by using an ELISA reader. *C*, in a cell-free system, coated uPA (20 nmol/liter) was incubated at 37 °C with Plg (50 nmol/liter) and substrate S-2251 (0.8 mmol/liter) in a 96-well plate. The reactions were performed as in *B*. The experiments in *B* and *C* were performed at least in triplicates, and results are representative of two independent experiments. *D*, uPA, coated as in *C*, was incubated with purified Plg (50 nmol) in the presence of aprotinin (2.5 μg/ml) and the indicated concentrations of LF. Bound material was analyzed by immunoblotting (*IB*). Results are representative of three independent experiments. *E*, the Plg activation assays were performed as in *C*, but SK was coated instead of uPA (20 nmol/liter). The reactions were performed in the presence of LF as indicated. *F*, the Plg activation assays were performed as in *C* in the presence of TF at the indicated concentrations. The experiments were performed at least in triplicates, and results are representative of three independent experiments: *, $p < 0.05$; **, $p < 0.005$. *Error bars*, S.D.

By using SPR, we determined the dissociation constant of the Plg-LF interaction to be 69 ± 24 nM and the IC_{50} of LF in inhibiting Plg activation to be 43 nM. These measures are similar yet somewhat higher than the concentrations of LF in human serum, which range from 5 to 30 nM in healthy donors (51, 52).[3] This suggests that under normal conditions, Plg activation would not be blocked by LF. However, LF concentrations might be up-regulated in site-specific microenvironments (*e.g.* upon degranulation of neutrophils) (7, 53). Further, high levels of LF were reported to be secreted by apoptotic cells (54). In apoptosis, LF might be necessary to down-regulate extracellular plasmin activity to avoid unwanted degradation of the surrounding tissue, inappropriate cell migration, or activation of proenzymes. The serum levels of LF might further increase during pregnancy (55). Thus, an anti-fibrinolytic property of LF may provide an intriguing clue to the reported higher risk of thromboembolism during pregnancy (56, 57).

The physiological relevance of the LF-Plg complex is indicated by the fact that we were able to coimmunoprecipitate both proteins from human serum. The SPR profile of the LF-Plg interaction suggests a two-state model with metastable initial complex 1 and stable complex 2. Time-dependent stabilization of the LF-Plg interaction may have important physiological

[3] A. Zwirzitz, M. Reiter, R. Skrabana, A. Ohradanova-Repic, O. Majdic, M. Gutekova, O. Cehlar, E. Petrovčíková, E. Kutejova, G. Stanek, H. Stockinger, and V. Leksa, unpublished data.

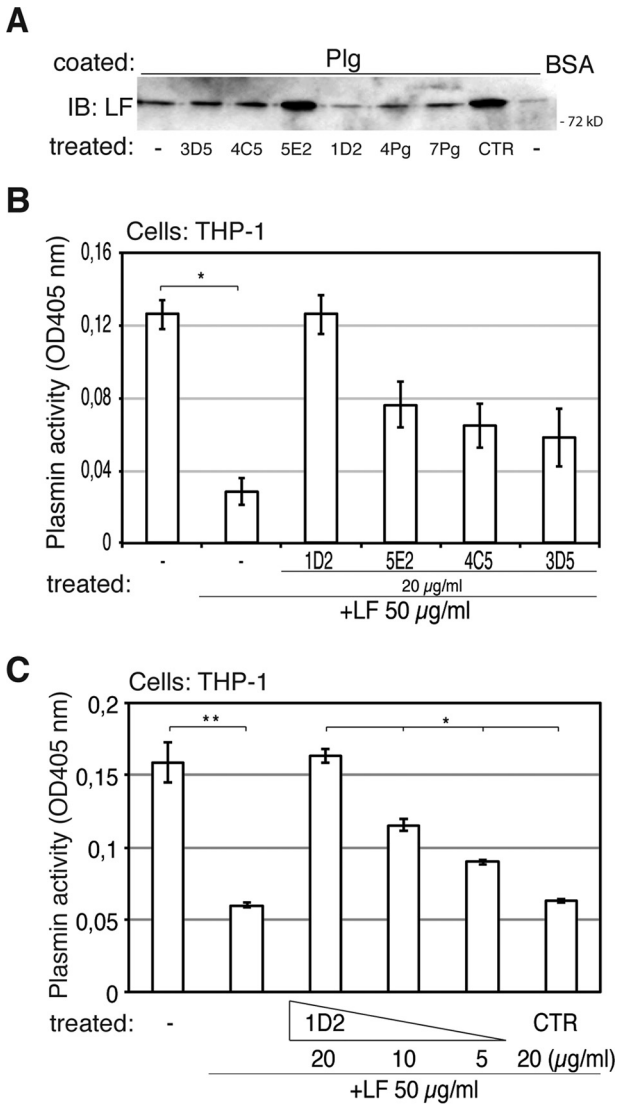

Figure 5. Reconstituting effect of the anti-LF mAb on Plg activation. *A*, the binding assay was performed as in Fig. 2*B*, but in the presence of various anti-LF mAbs (3D5, 4C5, 5E2, and 1D2) and anti-Plg mAbs (4Pg and 7Pg), all at 10 μg/ml. As an isotype control (*CTR*) mAb, we used AFP-01 against α-fetoprotein (10 μg/ml). *B* and *C*, plasminogen activation assays were performed as in Fig. 4*B*, but Plg was pre-incubated for 30 min on ice with or without the indicated concentrations of anti-LF mAb. *Error bars*, S.D.

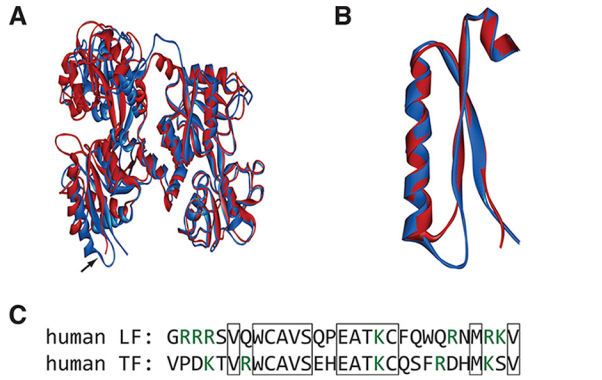

Figure 6. Structure comparison of LF and TF. *A*, superimposed structure of LF (*red*; real structure; PDB code 1LFG (19)) with TF (*blue*; real structure; PDB 3QYT (62)). The superimposed part covers 441 Cα atoms with a 1.2-Å root mean square deviation. *Arrow*, distinctions within N-terminal parts. *B*, comparison of the N-terminal part of LF corresponding to the antimicrobial peptide LFC (*red*; partial structure; PDB code 1LFG (19), residues Gly^{1}–Ala^{48}) with consonant part of transferrin (*blue*; partial structure; PDB code 3QYT (62), residues Val^{1}–Ala^{51}). The superimposed part covers 45 Cα atoms with a 0.88-Å root mean square deviation. *C*, sequence comparison of the N-terminal parts of human LF and TF. The *boxed* residues are identical, the *green* residues are positively charged.

consequences in situations where prolonged elevated levels of interacting proteins occur. Our data further suggest that the LF dimerization status, rather than its iron saturation, might modulate its capacity to interact with Plg.

In summary, LF intrinsically inhibits Plg activation through blocking the interaction between Plg and uPA. Thus, LF represents a novel pathway and tool to regulate plasmin-dependent functions.

Experimental procedures

Materials

Ammonium persulfate, TEMED, SDS, acrylamide, and *N*,*N*′-methylenebis-acrylamide were purchased from SERVA (Heidelberg, Germany). Human uPA and Glu-Plg were products of Calbiochem (Darmstadt, Germany). BSA was from Carl Roth (Karlsruhe, Germany). Lactoferrin, streptokinase, aprotinin (inhibitor of serine proteases), α2-antiplasmin (inhibitor of plasmin), Polybrene, mannose 1-phosphate, mannose 6-phosphate, all protease inhibitors, puromycin, tranexamic acid, and monensin were from Sigma-Aldrich. Beriglobin was from CSL Behring (King of Prussia, PA). Nonidet P-40 and Triton X-100 were obtained from Pierce. Plasmin-specific substrate S-2251 was a product of CoaChrom Diagnostica (Vienna, Austria). The streptavidin-HRP conjugate was supplied by GE Healthcare (Uppsala, Sweden). The LF-derived peptides were synthesized by Peptide 2.0 (Chantilly, VA). Human serum samples were obtained from healthy donors after informed consent that a part of the routine blood samples would be used for research purposes (approved by the Ethical Committee of the Medical University of Vienna). The study abides by the Declaration of Helsinki principles. All samples were stored at −20 °C before use.

Antibodies

The mAb MEM-238 to M6P/IGF2R was generated by us and produced by and purchased from EXBIO (Prague, Czech Republic); it was biotinylated or fluorescently conjugated by us. The AFP-01 mAb was generously provided by Dr. Václav Hoøejší (Institute of Molecular Genetics, Academy of Sciences of the Czech Republic, Prague, Czech Republic). mAbs to human LF (LF5-1D2, LF65-3D5, LF95-4C5, and LF124-5E2) were generated in the laboratory of Otto Majdic. Both biotinylated and FITC-conjugated rabbit polyclonal Ab to LF were purchased from Abcam (Cambridge, UK), and the mAbs to Plg (7Pg and 4Pg) were from Technoclone (Vienna, Austria). The goat anti-mouse IgG secondary antibody, both unlabeled and HRP-conjugated, was from Sigma-Aldrich. Goat anti-mouse IgG + IgM (H+L)-FITC conjugate was from An der Grub (Kaumberg, Austria); the anti-mouse IgG conjugates labeled fluorescently with Alexa Fluor 488 or Alexa Fluor 647 (AF647) were from Molecular Probes (Invitrogen).

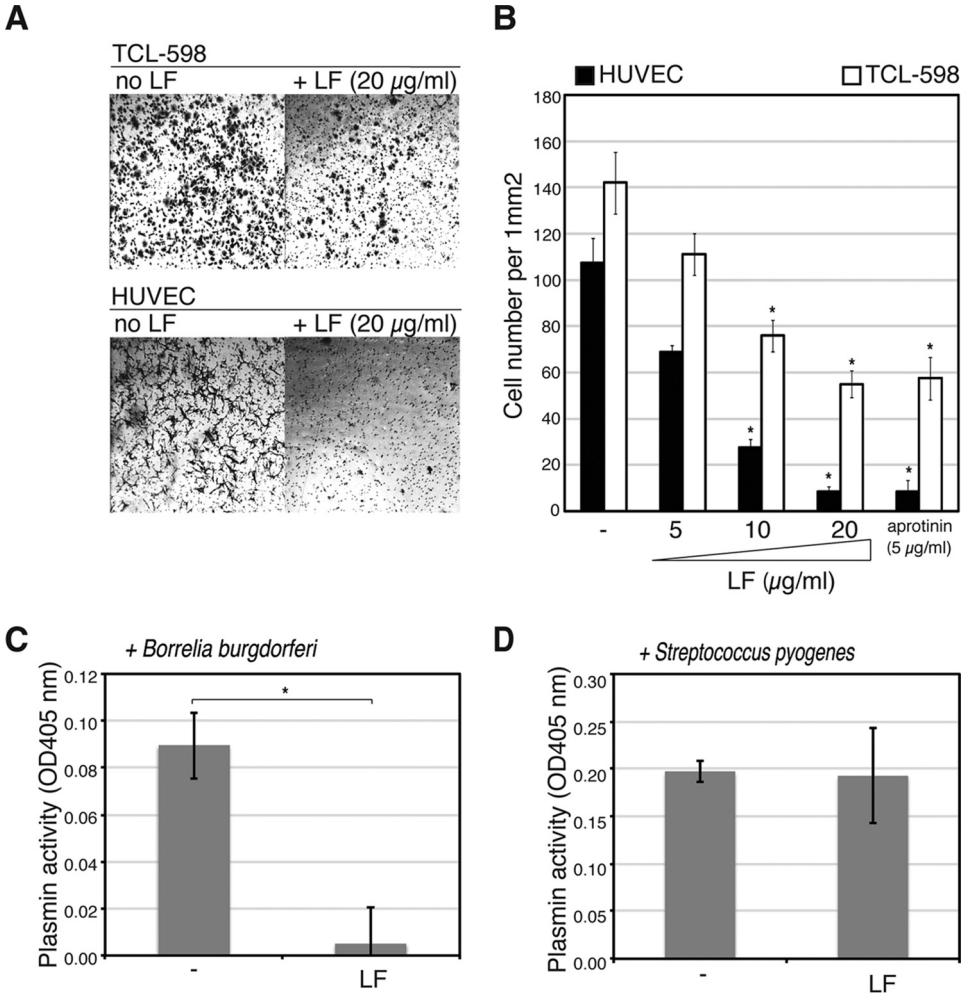

Figure 7. The effect of LF on patho/physiological functions of the Plg system. *A*, Matrigel-coated membranes of Boyden chambers were pre-incubated or not with the indicated concentrations of LF or aprotinin. Either epidermal growth factor (10 ng/ml) or vascular endothelial growth factor (10 nmol/liter) was added into the lower chambers to induce migration of the TCL-598 cells or HUVECs, respectively. The cells were seeded into the upper part of the filter (1×10^5 cells/filter) and incubated for 8 h at 37 °C. The cells that invaded the lower side of the filters were fixed and stained with crystal violet. Representative phase-contrast pictures of crystal violet–stained cells are shown. *B*, the numbers of cells that invaded onto the lower side of the filters were evaluated. *C*, *B. burgdorferi* sensu stricto B31 were incubated in human serum (40× diluted in PBS) in the presence of plasmin substrate S-2251 and LF. *D*, *S. pyogenes* were incubated in human serum (40× diluted in PBS) in the presence S-2251 and LF. In *C* and *D*, the basal level of Plg activation measured only with human serum without bacteria was subtracted. The experiments in *C* and *D* were performed at least in triplicates, and results are representative of three independent experiments; *, $p < 0.05$; **, $p < 0.005$. *Error bars*, S.D.

Cells

The human monocytic cell line THP-1 was from ATCC, and the human kidney epithelial tumor cell line TCL-598 was obtained from the Novartis Research Institute (Vienna, Austria). The cell lines were cultured in RPMI 1640 medium (Gibco/Invitrogen) supplemented with 100 units/ml penicillin, 100 μg/ml streptomycin, 2 mM L-glutamine and 10% heat-inactivated FCS (Sigma). All the cells were grown in a humidified atmosphere at 37 °C and 5% CO_2 and passaged suitably using trypsin-EDTA solution. Peripheral blood was separated into plasma, peripheral blood mononuclear cells, and granulocytes with red blood cells using the Lymphoprep gradient centrifugation (Axis Shield, Oslo, Norway), the latter followed by red cell lysis using aqua test.

Bacteria

S. pyogenes type strain was obtained from the Leibniz Institute DSMZ-German Collection of Microorganisms and Cell Cultures (DSMZ number 20565) and grown in brain–heart infusion broth (Carl Roth, Karlsruhe, Germany) at 37 °C. Bacterial growth was observed by absorbance at 600 nm (A_{600}) and was correlated to cfu/ml by plating on Columbia blood agar plates (bioMérieux, Vienna, Austria). An overnight culture of the bacteria was inoculated to fresh brain–heart infusion broth at an A_{600} of 0.05 and grown at 37 °C until it reached an A_{600} of 0.47 ($\sim 1 \times 10^8$ cfu/ml). Bacteria were pelleted at 6,000 × *g* for 10 min at room temperature and resuspended in sterile PBS for use in the experiment.

B. burgdorferi sensu stricto strain B31 was obtained from the Leibniz Institute DSMZ-German Collection of Microorganisms and Cell Cultures (DSMZ number 4680). *Borrelia* were grown in a modified BSK II medium as described (58). They were grown to logarithmic phase and enumerated using a counting chamber. The respective amount of culture was centrifuged at 6,000 × *g* for 10 min at room temperature, and the resulting pellet was washed once with 1 ml of sterile PBS. Sub-

sequently, the bacteria were brought up to a density of $4 \times 10^5/\mu$l in fresh PBS, and 25 μl (containing 10^7 spirochetes) were added to each reaction.

Flow cytometry and cell surface–binding assay

Cells were harvested, washed with PBS containing 1% BSA and 0.02% sodium azide, blocked with 2% beriglobin for 15 min on ice, and afterward incubated for 30 min on ice with specific mAb, either fluorescently labeled or unlabeled. For the latter, a second step staining was done with FITC-conjugated F(ab′)2 anti-mouse IgG+IgM antibodies. Before analysis, the cells were washed again. Apoptotic and necrotic cells were discriminated by staining with 7-aminoactinomycin D and the annexin V-PE conjugate (BD Biosciences). Then the analysis was carried on as described above. Flow cytometry was performed with an LSRII flow cytometer (BD Biosciences). Data acquisition was executed with the FACS DIVA software. Data analysis was accomplished with the FlowJo software (Treestar Inc., Ashland, OR).

To measure Plg binding to cells, the Plg molecule labeled with either Alexa Fluor 488 or AF647 (10 μg/ml), prepared in our laboratory, was pre-incubated on ice for 30 min with or without LF in PBS at the indicated concentrations. In parallel, THP-1 cells were harvested, washed, and then incubated on ice for 20 min with the Plg preparations at the indicated concentrations. Afterward, the cells were washed with PBS, and cell surface–bound Plg was analyzed by flow cytometry.

RNAi

The stable knockdown for M6P/IGF2R in THP-1 was generated by the delivery of a short hairpin RNA expression cassette as described in detail (10, 11).

Trypsin in-gel digestion and LC-MS/MS analysis

The 80 kDa Coomassie-stained gel band containing proteins co-purified with M6P/IGF2R was cut and destained with a mixture of methanol and 50 mM ammonium hydrogen carbonate. Proteins were reduced by DTT, alkylated by iodoacetamide, and treated with trypsin in cleavage buffer (100 mM Tris-HCl, pH 8.0, 1 mM $CaCl_2$, 10% acetonitrile). The digestion was carried out overnight at 37 °C and stopped by formic acid (1%). Peptide extraction was performed using TFA (0.1%) for the analysis. The HPLC system used was from the UltiMate™ system (Dionex Corp., Sunnyvale, CA) equipped with a PepMap C18 purification column (300 μm × 5 mm) and a 75 μm × 150-mm analytical column of the same material. The peptides were loaded on LC Packings "Switchos" module (Dionex) and a linear gradient (5–80%) of acetonitrile in formic acid (0.1%) was used for the elution. The LC-MS/MS analyses were carried out with the UltiMate™ system interfaced to an LTQ linear ion trap mass spectrometer (Thermo, San Jose, CA). The nanospray source of Proxeon (Odense, Denmark) was used with the distal coated silica capillaries of New Objective (Woburn, MA) at a voltage of up to 1500 V. Peptide spectra were recorded over the mass range of m/z 450–1600, and MS/MS spectra were recorded in information-dependent data acquisition over the mass range of m/z 200–2000. One full spectrum was recorded, followed by 4 MS/MS spectra, automatic gain control was applied, and the collision energy was set to the arbitrary value of 35 as collision gas. MS/MS spectra were interpreted by Mascot (Matrix Science Ltd., London, UK), peptide tolerance was set to ±2 Da, and MS/MS tolerance was set to ±0.8 Da, by using the nr (nonredundant) protein database (NCBI Resources, National Institutes of Health, Bethesda, MD). Proteins identified by the MASCOT search were inspected to create a protein list. The whole analysis was performed by the Mass Spectrometry Facility, Medical University of Vienna, Vienna, Austria.

Protein purification

M6P/IGF2R was isolated from THP-1 cells on cyanogen bromide–activated Sepharose 4B (Uppsala, Sweden) conjugated with the anti-M6P/IGF2R mAb MEM-238. The cells were lysed in lysis buffer containing 20 mM Tris-HCl (pH 8.2), 140 mM NaCl, 1% Nonidet P-40 detergent, and a mixture of protease inhibitors (10 μg/ml aprotinin, 10 μg/ml leupeptin, 1 mM phenylmethylsulfonyl fluoride, 100 nM N^{α}-*p*-tosyl-L-lysine chlormetylketone, 100 nM *N*-CBZ-L-phenylalanine chloromethyl ketone, 1 mM pepstatin A) for 30 min on ice. The lysate was clarified by centrifugation at 2,000 × *g* for 30 s at 4 °C and loaded onto the column. The column was washed with lysis buffer (3× volume). The elution was performed using the lysis buffer under stepwise increase of the pH (9.0, 10.0, and 11.7). After elution, the samples were immediately neutralized by adjusting the pH to 7.0 using HCl. Afterward, the fractions were analyzed by SDS-PAGE followed by immunoblotting or Coomassie Blue gel staining. By using a uPA-conjugated agarose column, soluble uPAR was isolated as described previously (59) from the conditioned medium of CHO cells expressing recombinant soluble uPAR. Purified proteins were optionally used in *in vitro* binding assays.

In vitro binding assay

For the binding assay, various molecules solubilized in PBS (pH 8.7) at a concentration of ~5 μg/ml were coated on wells of a 96-well BD Falcon™ plate for 2 h at 37 °C. Then the wells were blocked with 1% BSA in PBS for 1 h at room temperature and washed two times with binding buffer (20 mM Tris-HCl, 140 mM NaCl, pH 7.5). The wells were incubated for 4 h on ice with binding buffer supplemented with purified assayed proteins (~5 μg/ml) in the absence or presence of additional molecules and afterward washed two times with ice-cold binding buffer. Bound material was analyzed by SDS-PAGE and immunoblotting.

Immunoprecipitation

For immunoprecipitation, a 96-well BD Falcon™ plastic U-bottom plate was coated with goat anti-mouse IgG (5 μg/ml in PBS, pH 8.7) for 2 h at 37 °C. The plate was washed twice with PBS, incubated with specific antibodies (10 μg/ml in PBS) for 2 h at 37 °C, blocked with 1% BSA in PBS for 1 h at 37 °C, and washed twice with cold lysis buffer. Granulocytes were lysed for 30 min on ice with 1% Triton X-100 together with 0.5% dodecyl maltoside in 20 mM sodium phosphate buffer (pH 7.4) with a mixture of protease inhibitors and benzonase (Merck, Darmstadt, Germany; 50 units/

ml). Afterward, the lysate was passed twice through a needle (25 gauge). The lysate was clarified by centrifugation at 2,000 × *g* for 30 s at 4 °C. The supernatant, or in some experiments human serum, was loaded into the wells (50 μl/well) and incubated for 4 h at 4 °C. Then the wells were washed four times with cold lysis buffer, and the precipitates were collected with sample buffer and analyzed using SDS-PAGE followed by immunoblotting.

Electrophoresis and immunoblotting

Samples obtained from cell lysis, protein purification, *in vitro* binding assays, *in vitro* proteolysis assay, or immunoprecipitation analysis were analyzed by electrophoresis on an appropriate SDS-polyacrylamide gel, followed by a transfer at constant voltage (15 V) to Immobilon polyvinylidene difluoride membranes (Millipore Co., Bedford, MA). The membranes were blocked using 4% nonfat milk and immunostained with specific mAb. For visualization of proteins, the chemiluminescence image analyzer FUJIFILM/LAS-4000 was used.

BN-PAGE

As described in detail elsewhere (12), in the first dimension, a native separation gel was used. Ferritin (monomer (440 kDa) and dimer (880 kDa)), jack bean urease (monomer (91 kDa), trimer (272 kDa), and hexamer (545 kDa)) and BSA (all from Sigma) were used as markers. The serum samples were loaded as described (12), and electrophoresis was performed at 80 V and room temperature overnight. The following day, the lanes were cut from the gel, put on the top of a second-dimension SDS-polyacrylamide gel, and run at room temperature overnight. Afterward, the gel was blotted onto a Immobilon polyvinylidene difluoride membrane, and the membrane was blocked with 4% milk and then incubated with specific antibodies for visualization.

Plasminogen activation assay

For the analysis of Plg activation in a cell-free system, uPA or SK (10 nM) in PBS (pH 8.7) was coated on a 96-well Falcon plate for 2 h at 37 °C. The wells were blocked with 1% BSA in PBS for 1 h at room temperature, washed two times with PBS, and afterward incubated at 37 °C in PBS with human Glu-Plg (50 nM) and the chromogenic plasmin substrate (S-2251; 0.8 mM).

For the analysis of Plg activation at the cell surface, the cells were washed twice with serum-free RPMI 1640 medium and afterward incubated at 37 °C in serum-free medium together with human Glu-Plg (50 nM) and S-2251 in a 96-well plate (5×10^5 cells/well). The absorbance change at 405 nm was monitored at different time points by using an ELISA reader (SpectraMax M5, Molecular Devices). To block the activity of unbound plasmin and to study Plg activation at the cell surface only, the assays were performed in the presence of α2-antiplasmin (2.5 μg/ml). Optionally, various substances were added to the reaction.

For the analysis of Plg activation by bacteria, a 2× master mix containing BSA (final concentration, 2 μg/ml), Plg (50 nM), and the chromogenic substrate S-2251 (0.8 mM) diluted in PBS was prepared. Bacteria were added to the master mix (5×10^7 cfu/ml in the case of *S. pyogenes* and 1×10^7 cfu/ml for *Borrelia*). Aliquots without bacteria were used as controls. Finally, the reaction volume was made up to 100 μl with PBS. Tubes were shaken at 37 °C overnight, and the color change was measured in triplicate using an EL 808 microplate reader (BioTek, Bad Friedrichshall, Germany). The basal level of Plg activation measured only with human serum without bacteria was subtracted.

Cell invasion assay

The invasion of both TCL-598 cells and HUVECs was measured by an assay based on the Boyden chamber principle with filter inserts containing 8-μm pore size polycarbonate membranes coated with basement membrane Matrigel matrix (BD Biosciences). Optionally, the Matrigel was pre-incubated with inhibitors (LF or aprotinin) diluted in serum-free medium for 1 h at 37 °C. Either epidermal growth factor (10 ng/ml) or vascular endothelial growth factor (50 ng/ml) in RPMI 1640 medium (10% FCS) was added into the lower chambers to induce migration of the TCL-598 cells or HUVECs, respectively. The cells were seeded into the upper part of the filter (1×10^5 cells/filter) and incubated for 8 h at 37 °C. Then the filters were removed, the upper surface of the membrane was scraped free of cells, and the number of cells invaded onto the lower side of the filters was evaluated after fixing and staining with crystal violet by counting.

Structure comparisons

All three-dimensional structures were retrieved from the Protein Data Bank (PDB) (60). Comparison of structures was carried out by Multiprot (61), and the structures were visualized by WebLabViewerLite (Molecular Simulations, Inc.). Superimposed structure of LF (real structure; PDB code 1LFG (19)) was compared with TF (real structure; PDB code 3QYT (62)). The superimposed part covered 441 Cα atoms with a 1.2-Å root mean square deviation. The N-terminal part of LF corresponding to the antimicrobial peptide LFC (partial structure; PDB code 1LFG (19), residues Gly^1–Ala^{48}) was compared with the corresponding part of transferrin (partial structure; PDB code 3QYT (62); residues Val^1–Ala^{51}). The superimposed part covers 45 Cα atoms with a 0.88 Å root mean square deviation.

Determination of binding by SPR

A Biacore 3000 instrument with a streptavidin Sensor Chip SA (GE Healthcare) was used. All experiments were performed at 25 °C in PBS (10 mM phosphate buffer, pH 7.2, 150 mM NaCl) with 0.005% Tween 20 as running buffer. For biotinylation, iron-saturated recombinant human LF (Sigma, L1294), 1.8 mg/ml in 0.1 M sodium acetate, pH 5.5, was treated with 10 mM sodium *meta*-periodate for 15 min on ice to introduce carbonyl groups on LF's glycans. Oxidized LF was buffer-exchanged using a desalting column equilibrated with PBS, giving 0.7 mg/ml LF solution. A DMSO stock solution of EZ-link hydrazide biotin (Thermo Scientific, 21339) was added to a 5 mM final concentration, and the mixture was incubated for 45 min at 25 °C. Unreacted ligand was removed on a desalting column

equilibrated with PBS. Biotinylated LF (~1 μg/ml) was immobilized on the SA sensor chip to a final level of 1400 response units. After sensor chip pretreatment with 100 mM HCl (see "Results" for details), serially diluted plasminogen (10–160 nM) was injected at a 30 μl/min flow rate, allowing an association and dissociation time of 60 and 120 s, respectively. Regeneration of the LF surface was accomplished by a 13-s injection of 10 mM HCl. Binding data were double-referenced (63), and the kinetic constants and affinity were derived from fitting a 1:1, two-state reaction model as implemented in BIAevaluation software version 4.1.1. Rate constants were approximated globally, maximal responses were fitted locally, and the bulk response was set to zero. The influence of the LF iron content on the binding of plasminogen was tested after iron resaturation with 10 μM iron(III) sulfate in 100 μM imidazole, pH 7.0, and 10 μM sodium bicarbonate.

Light-scattering measurements

LF solutions were centrifuged at 10,000 × *g* for 10 min, transferred into a 1-μl cuvette, and measured in a Dynapro NanoStar instrument controlled by Dynamics software version 7.7.0.125 (Wyatt Technology). Both DLS and static light-scattering data were collected from sample. Evaluation of data was performed by the Dynamics software. Adopting a globular protein model, DLS autocorrelation data were analyzed by a cumulant analysis with polydispersity calculation and a regularization analysis by the Dynals algorithm for characterization of average particle radius and high-molecular weight species, respectively. Static light scattering averaged intensity was used for molar mass calculation using a sphere model. To cull the acquisitions influenced by dust or irregular particles, an automatic filtering of autocorrelation functions was applied with a baseline threshold of 0.997–1.003 and a maximal allowed sum-of-squares error for cumulant fit equal to 10.

Statistical analysis

All experiments were performed at least three times in at least triplicates. The data were expressed as mean values with S.D. Statistical significance was evaluated by using Student's *t* test; values of $p < 0.05$ (*) and $p < 0.005$ (**) (as indicated) were considered to be significant or highly significant, respectively.

Author contributions—V. L. conceived and designed the experiments. V. L., A. Z., M. R., M. G., R. S., O. C., and E. P. performed experiments and analyzed data. R. S. contributed to the design of SPR and DLS experiments. H. S., A. O.-R., R. S., E. K., G. S., and O. M. contributed with ideas, comments, and materials. V. L. wrote the paper. All authors read and corrected the manuscript.

Acknowledgments—We thank S. Stewart for the lentiviral vector pLKOpuro1. We also thank Keiryn Bennett (CeMM, Vienna, Austria) for discussions on LC-MS/MS analysis.

References

1. Danø, K., Behrendt, N., Høyer-Hansen, G., Johnsen, M., Lund, L. R., Ploug, M., and Rømer, J. (2005) Plasminogen activation and cancer. *Thromb. Haemost.* **93,** 676–681 Medline
2. Dotti, C. G., Galvan, C., and Ledesma, M. D. (2004) Plasmin deficiency in Alzheimer's disease brains: causal or casual? *Neurodegener. Dis.* **1,** 205–212 CrossRef Medline
3. Doeuvre, L., Plawinski, L., Goux, D., Vivien, D., and Anglés-Cano, E. (2010) Plasmin on adherent cells: from microvesiculation to apoptosis. *Biochem. J.* **432,** 365–373 CrossRef Medline
4. Hu, L. T., Perides, G., Noring, R., and Klempner, M. S. (1995) Binding of human plasminogen to *Borrelia burgdorferi*. *Infect. Immun.* **63,** 3491–3496 Medline
5. Klempner, M. S., Noring, R., Epstein, M. P., McCloud, B., Hu, R., Limentani, S. A., and Rogers, R. A. (1995) Binding of human plasminogen and urokinase-type plasminogen activator to the Lyme disease spirochete, *Borrelia burgdorferi*. *J. Infect. Dis.* **171,** 1258–1265 CrossRef Medline
6. Wang, X., Lin, X., Loy, J. A., Tang, J., and Zhang, X. C. (1998) Crystal structure of the catalytic domain of human plasmin complexed with streptokinase. *Science* **281,** 1662–1665 CrossRef Medline
7. Legrand, D. (2016) Overview of lactoferrin as a natural immune modulator. *J. Pediatr.* **173,** S10–S15 CrossRef Medline
8. Vogel, H. J. (2012) Lactoferrin, a bird's eye view. *Biochem. Cell Biol.* **90,** 233–244 CrossRef Medline
9. Leksa, V., Godár, S., Cebecauer, M., Hilgert, I., Breuss, J., Weidle, U. H., Horejsí, V., Binder, B. R., and Stockinger, H. (2002) The N terminus of mannose 6-phosphate/insulin-like growth factor 2 receptor in regulation of fibrinolysis and cell migration. *J. Biol. Chem.* **277,** 40575–40582 CrossRef Medline
10. Schiller, H. B., Szekeres, A., Binder, B. R., Stockinger, H., and Leksa, V. (2009) Mannose 6-phosphate/insulin-like growth factor 2 receptor limits cell invasion by controlling αVβ3 integrin expression and proteolytic processing of urokinase-type plasminogen activator receptor. *Mol. Biol. Cell* **20,** 745–756 CrossRefMedline
11. Leksa, V., Pfisterer, K., Ondrovičová, G., Binder, B., Lakatošová, S., Donner, C., Schiller, H. B., Zwirzitz, A., Mrvová, K., Pevala, V., Kutejová, E., and Stockinger, H. (2012) Dissecting mannose 6-phosphate-insulin-like growth factor 2 receptor complexes that control activation and uptake of plasminogen in cells. *J. Biol. Chem.* **287,** 22450–22462 CrossRef Medline
12. Leksa, V., Loewe, R., Binder, B., Schiller, H. B., Eckerstorfer, P., Forster, F., Soler-Cardona, A., Ondrovicová, G., Kutejová, E., Steinhuber, E., Breuss, J., Drach, J., Petzelbauer, P., Binder, B. R., and Stockinger, H. (2011) Soluble M6P/IGF2R released by TACE controls angiogenesis via blocking plasminogen activation. *Circ. Res.* **108,** 676–685 CrossRef Medline
13. Sleat, D. E., Kraus, S. R., Sohar, I., Lackland, H., and Lobel, P. (1997) α-Glucosidase and *N*-acetylglucosamine-6-sulphatase are the major mannose-6-phosphate glycoproteins in human urine. *Biochem. J.* **324,** 33–39 CrossRef Medline
14. Sleat, D. E., Wang, Y., Sohar, I., Lackland, H., Li, Y., Li, H., Zheng, H., and Lobel, P. (2006) Identification and validation of mannose 6-phosphate glycoproteins in human plasma reveal a wide range of lysosomal and non-lysosomal proteins. *Mol. Cell. Proteomics* **5,** 1942–1956 CrossRef Medline
15. Gifford, J. L., Hunter, H. N., and Vogel, H. J. (2005) Lactoferricin: a lactoferrin-derived peptide with antimicrobial, antiviral, antitumor and immunological properties. *Cell. Mol. Life Sci.* **62,** 2588–2598 CrossRef Medline
16. Haney, E. F., Nazmi, K., Lau, F., Bolscher, J. G., and Vogel, H. J. (2009) Novel lactoferrampin antimicrobial peptides derived from human lactoferrin. *Biochimie* **91,** 141–154 CrossRef Medline
17. Miles, L. A., Hawley, S. B., Baik, N., Andronicos, N. M., Castellino, F. J., and Parmer, R. J. (2005) Plasminogen receptors: the sine qua non of cell surface plasminogen activation. *Front. Biosci.* **10,** 1754–1762 Medline
18. Leksa, V., Godar, S., Schiller, H. B., Fuertbauer, E., Muhammad, A., Slezakova, K., Horejsi, V., Steinlein, P., Weidle, U. H., Binder, B. R., and Stockinger, H. (2005) TGF-β-induced apoptosis in endothelial cells mediated by M6P/IGFII-R and mini-plasminogen. *J. Cell Sci.* **118,** 4577–4586 CrossRef Medline

19. Haridas, M., Anderson, B. F., and Baker, E. N. (1995) Structure of human diferric lactoferrin refined at 2.2 A resolution. *Acta Crystallogr. D Biol. Crystallogr.* **51,** 629–646 CrossRef Medline
20. Majka, G., Śpiewak, K., Kurpiewska, K., Heczko, P., Stochel, G., Strus, M., and Brindell, M. (2013) A high-throughput method for the quantification of iron saturation in lactoferrin preparations. *Anal. Bioanal. Chem.* **405,** 5191–5200 CrossRef Medline
21. Persson, B. A., Lund, M., Forsman, J., Chatterton, D. E., and Akesson, T. (2010) Molecular evidence of stereo-specific lactoferrin dimers in solution. *Biophys. Chem.* **151,** 187–189 CrossRef Medline
22. Kanyshkova, T. G., Babina, S. E., Semenov, D. V., Isaeva, N., Vlassov, A. V., Neustroev, K. N., Kul'minskaya, A. A., Buneva, V. N., and Nevinsky, G. A. (2003) Multiple enzymic activities of human milk lactoferrin. *Eur. J. Biochem.* **270,** 3353–3361 CrossRef Medline
23. Cederholm-Williams, S. A. (1981) Concentration of plasminogen and antiplasmin in plasma and serum. *J. Clin. Pathol.* **34,** 979–981 CrossRef Medline
24. Costello, M., Baxter, R. C., and Scott, C. D. (1999) Regulation of soluble insulin-like growth factor II/mannose 6-phosphate receptor in human serum: measurement by enzyme-linked immunosorbent assay. *J. Clin. Endocrinol. Metab.* **84,** 611–617 CrossRef Medline
25. Legrand, D., Elass, E., Carpentier, M., and Mazurier, J. (2005) Lactoferrin: a modulator of immune and inflammatory responses. *Cell Mol. Life Sci.* **62,** 2549–2559 CrossRef Medline
26. El-Shewy, H. M., and Luttrell, L. M. (2009) Insulin-like growth factor-2/mannose-6 phosphate receptors. *Vitam. Horm.* **80,** 667–697 CrossRef Medline
27. Young, K. C., Shi, G. Y., Wu, D. H., Chang, L. C., Chang, B. I., Ou, C. P., and Wu, H. L. (1998) Plasminogen activation by streptokinase via a unique mechanism. *J. Biol. Chem.* **273,** 3110–3116 CrossRef Medline
28. Lähteenmaki, K., Kuusela, P., and Korhonen, T. K. (2001) Bacterial plasminogen activators and receptors. *FEMS Microbiol. Rev.* **25,** 531–552 CrossRef Medline
29. Wally, J., and Buchanan, S. K. (2007) A structural comparison of human serum transferrin and human lactoferrin. *Biometals* **20,** 249–262 CrossRef Medline
30. van Hinsbergh, V. W., Engelse, M. A., and Quax, P. H. (2006) Pericellular proteases in angiogenesis and vasculogenesis. *Arterioscler. Thromb. Vasc. Biol.* **26,** 716–728 CrossRef Medline
31. Tarui, T., Majumdar, M., Miles, L. A., Ruf, W., and Takada, Y. (2002) Plasmin-induced migration of endothelial cells: a potential target for the anti-angiogenic action of angiostatin. *J. Biol. Chem.* **277,** 33564–33570 CrossRef Medline
32. Degryse, B. (2011) The urokinase receptor system as strategic therapeutic target: challenges for the 21st century. *Curr. Pharm. Des.* **17,** 1872–1873 CrossRef Medline
33. McArthur, J. D., Cook, S. M., Venturini, C., and Walker, M. J. (2012) The role of streptokinase as a virulence determinant of *Streptococcus pyogenes*: potential for therapeutic targeting. *Curr. Drug Targets* **13,** 297–307 CrossRef Medline
34. Gebbia, J. A., Monco, J. C., Degen, J. L., Bugge, T. H., and Benach, J. L. (1999) The plasminogen activation system enhances brain and heart invasion in murine relapsing fever borreliosis. *J. Clin. Invest.* **103,** 81–87 CrossRef Medline
35. Fuchs, H., Wallich, R., Simon, M. M., and Kramer, M. D. (1994) The outer surface protein A of the spirochete *Borrelia burgdorferi* is a plasmin(ogen) receptor. *Proc. Natl. Acad. Sci. U.S.A.* **91,** 12594–12598 CrossRef Medline
36. Brunetti, C. R., Burke, R. L., Kornfeld, S., Gregory, W., Masiarz, F. R., Dingwell, K. S., and Johnson, D. C. (1994) Herpes simplex virus glycoprotein D acquires mannose 6-phosphate residues and binds to mannose 6-phosphate receptors. *J. Biol. Chem.* **269,** 17067–17074 Medline
37. Hasegawa, K., Motsuchi, W., Tanaka, S., and Dosako, S. (1994) Inhibition with lactoferrin of *in vitro* infection with human herpes virus. *Jpn. J. Med. Sci. Biol.* **47,** 73–85 CrossRef Medline
38. Callé, A., Ugrinova, I., Epstein, A. L., Bouvet, P., Diaz, J. J., and Greco, A. (2008) Nucleolin is required for an efficient herpes simplex virus type 1 infection. *J. Virol.* **82,** 4762–4773 CrossRef Medline
39. Stillfried, G. E., Saunders, D. N., and Ranson, M. (2007) Plasminogen binding and activation at the breast cancer cell surface: the integral role of urokinase activity. *Breast Cancer Res.* **9,** R14 CrossRef Medline
40. Mangel, W. F., Lin, B. H., and Ramakrishnan, V. (1990) Characterization of an extremely large, ligand-induced conformational change in plasminogen. *Science* **248,** 69–73 CrossRef Medline
41. Bugge, T. H. (2008) *Physiological Functions of Plasminogen Activation: Effects of Gene Deficiences in Human and Mice*, pp. 183–201, Springer, New York
42. Lucas, M. A., Fretto, L. J., and McKee, P. A. (1983) The binding of human plasminogen to fibrin and fibrinogen. *J. Biol. Chem.* **258,** 4249–4256 Medline
43. Plow, E. F., Freaney, D. E., Plescia, J., and Miles, L. A. (1986) The plasminogen system and cell surfaces: evidence for plasminogen and urokinase receptors on the same cell type. *J. Cell Biol.* **103,** 2411–2420 CrossRef Medline
44. Boxrud, P. D., and Bock, P. E. (2000) Streptokinase binds preferentially to the extended conformation of plasminogen through lysine binding site and catalytic domain interactions. *Biochemistry* **39,** 13974–13981 CrossRef Medline
45. Reed, G. L., Lin, L. F., Parhami-Seren, B., and Kussie, P. (1995) Identification of a plasminogen binding region in streptokinase that is necessary for the creation of a functional streptokinase-plasminogen activator complex. *Biochemistry* **34,** 10266–10271 CrossRef Medline
46. Verhamme, I. M., and Bock, P. E. (2014) Rapid binding of plasminogen to streptokinase in a catalytic complex reveals a three-step mechanism. *J. Biol. Chem.* **289,** 28006–28018 CrossRef Medline
47. Binder, B. R., and Mihaly, J. (2008) The plasminogen activator inhibitor "paradox" in cancer. *Immunol. Lett.* **118,** 116–124 CrossRef Medline
48. Wiman, B., and Collen, D. (1979) On the mechanism of the reaction between human α2-antiplasmin and plasmin. *J. Biol. Chem.* **254,** 9291–9297 Medline
49. Wiman, B., Lijnen, H. R., and Collen, D. (1979) On the specific interaction between the lysine-binding sites in plasmin and complementary sites in α2-antiplasmin and in fibrinogen. *Biochim. Biophys. Acta* **579,** 142–154 CrossRef Medline
50. Lijnen, H. R., Van Hoef, B., and Collen, D. (1981) On the role of the carbohydrate side chains of human plasminogen in its interaction with α 2-antiplasmin and fibrin. *Eur. J. Biochem.* **120,** 149–154 CrossRef Medline
51. Bennett, R. M., and Kokocinski, T. (1979) Lactoferrin turnover in man. *Clin. Sci.* **57,** 453–460 CrossRef Medline
52. Német, K., Solti, V., Mód, A., Pálóczi, K., Szegedi, G., and Hollán, Z. (1987) Plasma lactoferrin levels in leukaemias. *Clin. Lab. Haematol.* **9,** 137–145 CrossRef Medline
53. Mayeur, S., Spahis, S., Pouliot, Y., and Levy, E. (2016) Lactoferrin, a pleiotropic protein in health and disease. *Antioxid. Redox Signal.* **24,** 813–836 CrossRef Medline
54. Bournazou, I., Pound, J. D., Duffin, R., Bournazos, S., Melville, L. A., Brown, S. B., Rossi, A. G., and Gregory, C. D. (2009) Apoptotic human cells inhibit migration of granulocytes via release of lactoferrin. *J. Clin. Invest.* **119,** 20–32 Medline
55. Baynes, R. D., Lamparelli, R. D., Bezwoda, W. R., Dajee, D., and van der Walt, L. A. (1989) Plasma lactoferrin content in pregnancy. *S. Afr. Med. J.* **76,** 531–534 Medline
56. Brenner, B. (2004) Haemostatic changes in pregnancy. *Thromb. Res.* **114,** 409–414 CrossRef Medline
57. Bremme, K. A. (2003) Haemostatic changes in pregnancy. *Best Pract. Res. Clin. Haematol.* **16,** 153–168 CrossRef Medline
58. Reiter, M., Schötta, A. M., Müller, A., Stockinger, H., and Stanek, G. (2015) A newly established real-time PCR for detection of *Borrelia miyamotoi* in Ixodes ricinus ticks. *Ticks Tick Borne Dis.* **6,** 303–308 CrossRef Medline
59. Magdolen, V., Rettenberger, P., Lopens, A., Oi, H., Lottspeich, F., Kellermann, J., Creutzburg, S., Goretzki, L., Weidle, U. H., and Wilhelm, O.

(1995) Expression of the human urokinase-type plasminogen activator receptor in *E. coli* and Chinese hamster ovary cells: purification of the recombinant proteins and generation of polyclonal antibodies in chicken. *Electrophoresis* **16,** 813– 816 CrossRef Medline

60. Berman, H. M., Westbrook, J., Feng, Z., Gilliland, G., Bhat, T. N., Weissig, H., Shindyalov, I. N., and Bourne, P. E. (2000) The Protein Data Bank. *Nucleic Acids Res.* **28,** 235–242 CrossRef Medline
61. Shatsky, M., Nussinov, R., and Wolfson, H. J. (2004) A method for simultaneous alignment of multiple protein structures. *Proteins* **56,** 143–156 CrossRef Medline
62. Yang, N., Zhang, H., Wang, M., Hao, Q., and Sun, H. (2012) Iron and bismuth bound human serum transferrin reveals a partially-opened conformation in the N-lobe. *Sci. Rep.* **2,** 999 CrossRef Medline
63. Myszka, D. G. (1999) Improving biosensor analysis. *J. Mol. Recognit.* **12,** 279 –284 CrossRef Medline
64. Sittampalam, S., Coussens, N. P., Brimacombe, K., Grossman, A., Arkin, M., Auld, D., Austin, C., Baell, J., Bejcek, B., Chung, T. D. Y., Dahlin, J. L., Devanaryan, V., Foley, T. L., Glicksman, M., Hall, M. D., *et al.* (2017) *Assay Guidance Manual*, version 5.0, Eli Lilly and Company and NIH Chemical Genomics Center, Bethesda, MD